Reviewer #1 Comments:

We thank the reviewer for the constructive comments. In the following, we repeat the reviewer's comments in black and insert our answers in blue. In some cases, we highlight the changes made in the manuscript, written in italic font whereas the original text is repeated with grey coloring.

This study estimates methane emissions in a key region where greenhouse gas emissions and satellite data have considerable biases. This uncertainty, along with the proportion of emissions from this region to the global burden, makes it a target for mitigation efforts. Regional emission estimates, therefore, are important in that direction. This manuscript is written concisely but needs some additional points. Key analysis to add includes a validation with independent data, as satellite data have been known to have biases in this region. Monsoon seasonality in emissions related to rain-fed agriculture or wetlands is expected, but how robust the estimate/conclusion should be shown with posterior statistics, with independent observations in this region. Also, the focus should be on the whole domain (the abstract also lacks that- e.g., what causes the seasonality for the whole domain), instead of projecting the LIB result as a key result. After addressing the comments, this manuscript may be considered for publication.

We thank the reviewer for this constructive comment and fully agree that validation with independent observations is, in principle desirable, particularly given the known challenges and potential biases of satellite methane retrievals over South Asia.

Independent validation

There is currently no publicly available dataset of ground-based observations for this region that we are aware of. To our knowledge, there is no data sets that are both (i) available for the study period and have good quality and (ii) have sufficiently regionally representative (not within an urban area) to provide a meaningful validation of our posterior emission estimates. Existing in-situ measurements in South Asia are extremely sparse and are often located in or near urban environments, making them poorly representative of the large-scale, predominantly agricultural and wetland emission regions that dominate our inversion domain. Much of in-situ data from the region is not openly accessible, limiting its use for independent validation.

To address this, now we have used the GOSAT-TROPOMI blended dataset (Balasus et al., 2023) to test our results. This dataset applies machine-learning-based bias correction and is developed independently of the WFMD TROPOMI retrievals used in our inversion. A new section now compares posterior model concentrations against this dataset, showing consistent seasonal behavior and improved agreement relative to the prior simulation. The corresponding figures and evaluation are provided at the end of this document for reference.

Robustness of posterior emissions

In addition to the sensitivity tests to the error assumptions, we now conducted sensitivity experiments by strongly perturbing prior flux magnitudes (~33–133 Tg CH_4 yr^{-1}). Despite these large changes, posterior emissions converge to a narrow range (~65–73 Tg CH_4 yr^{-1}) with consistent spatial and seasonal patterns. This indicates that the inversion is not strongly controlled by the absolute magnitude of the prior emissions and that the national-scale posterior estimates are relatively robust.

Domain-wide focus and seasonality

The processes driving the seasonality are different in different regions, and we therefore keep the separate discussions on the subregions. We believe that this is also an important validation aspect, since the seasonality can be understood in terms of run-off data for the different river basins. The fact that we do see different seasonality of methane emissions in the LIB, where the river flow is also driven by snow melt, compared to the Bangladesh region, where the river flow is more directly controlled by the monsoon, corroborates the validity of our seasonal emission patterns.
Together these analyses indicate that our estimates are robust and the satellite observations provide meaningful constraint on methane emissions at the national scale for South Asia in 2020.

Specific points

Abstract

"Agriculture and wetlands contribute substantially to the regional budget,..". Better to be quantitative here. You have analyzed climatic factors in the South Asian domain as well. Better to reflect those aspects in the abstract also.

Agriculture and wetlands contribute substantially to the regional budget, with the flux increments coincident with rice-growing areas and inundated lowlands. The inversion indicates pronounced monsoon-modulated seasonality: posterior fluxes are higher than the prior during June–September by ~70% and lower during January–May by ~46%.

We changed the text to:

Agriculture and wetlands contribute substantially to the regional budget, with the flux increments coincident with rice-growing areas and inundated lowlands. The inversion indicates pronounced monsoon-modulated seasonality in South Asia: posterior fluxes are higher than the prior by about 19.3 Tg CH_4 (an increase of ~70%) during June–September and lower during January–May by ~46%.

Introduction

26-27: "Methane (CH_4) is a potent greenhouse gas with a global warming potential 85 times higher than that of carbon dioxide over a 20-year period." Reference needed

Methane (CH_4) is a potent greenhouse gas with a global warming potential 85 times higher than that of carbon dioxide over a 20-year period.

Changed to:

Methane (CH_4) is a potent greenhouse gas with a global warming potential 84-87 times higher than that of carbon dioxide over a 20-year period (International Energy Agency, 2021).

59-60: include basic references for SCIAMACHY, GOSAT, etc., and give credit to the Agency behind the effort

The earliest satellite observations for methane were provided by the SCanning Imaging Absorption spectroMeter for Atmospheric CHartographY (SCIAMACHY) instrument onboard the ENVISAT satellite, launched in 2002. The launch of the first dedicated greenhouse gas monitoring satellite, GOSAT (Greenhouse Gases Observing Satellite), in 2009 opened the possibility for monitoring carbon dioxide and methane emissions across the globe. Since then, several other satellites have enhanced the GHG monitoring capabilities. The TROPOspheric Monitoring Instrument (TROPOMI) on the Sentinel-5 Precursor satellite, launched in October 2017, provides high-resolution, daily global observations of atmospheric methane. The TROPOMI data offer unprecedented spatial and temporal coverage well suited for GHG estimation both on global and regional scales.

Changed to:

The earliest satellite observations for methane were provided by the SCanning Imaging Absorption spectroMeter for Atmospheric CHartographY (SCIAMACHY) instrument onboard the European Space Agency's (ESA) ENVISAT satellite, launched in 2002 (Bovensmann et al., 1999). The launch of the first dedicated greenhouse gas monitoring satellite, GOSAT (Greenhouse Gases Observing Satellite) with its TANSO-FTS instrument developed by JAXA, in 2009 opened the possibility for monitoring carbon dioxide and methane emissions across the globe (Kuze et al., 2009). Since then, several other satellites have enhanced the GHG monitoring capabilities (Jacob et al., 2022). The TROPOspheric Monitoring

Instrument (TROPOMI) on the ESA's Sentinel-5 Precursor satellite, launched in October 2017, provides high-resolution, daily global observations of atmospheric methane (Hu et al., 2016). The TROPOMI data offer unprecedented spatial and temporal coverage well suited for GHG estimation both on global and regional scales.

Connect the last two paragraphs of page 2 on the sparsity of surface networks to the use of satellites

Thank you for the comment, we joined the two paragraphs.

Added:

In this context, satellite observations provide the essential alternative (Streets et al., 2013), capable of delivering spatially continuous and regionally representative methane measurements, making them indispensable for top-down emission estimation in regions such as South Asia.

Also mention some studies on the biases in satellite products over Asia, then the biases in TROPOMI early products, and how this product is better.

Satellite retrievals of methane are known to have systematic biases that vary by instrument, retrieval methodology and region, driven by factors such as surface albedo, aerosols, and thin clouds. Over Asia, these effects have been shown to translate into substantial differences in inferred emissions, with GOSAT and TROPOMI based inversions differing by up to 7.7 Tg yr^{-1} over northern India and eastern China (Liang et al., 2023). Biases associated with surface reflectance, aerosol loading, and across-track striping in early TROPOMI products can exceed 10 ppb in some regions and have been linked to false methane anomalies caused by unmodelled surface spectral features or inadequate topographic information (Balasus et al., 2023; Jongaramrungruang et al., 2021; Lorente et al., 2023). Algorithm updates to the operational TROPOMI retrieval have substantially reduced albedo-dependent biases through improved spectroscopy, higher-resolution surface altitude data, and posteriori corrections (Lorente et al., 2021). The scientific TROPOMI WFMD product further addresses these issues by using higher-order polynomial fitting to better represent spectral albedo variability, updated digital elevation models, refined machine-learning based quality filtering, and orbit-wise destriping and calibration, resulting in reduced systematic errors and improved spatiotemporal consistency. Notably, persistent seasonal biases present in the operational product at high latitudes are largely absent in WFMD (Lindqvist et al., 2024; Schneising et al., 2023).

Data and methods

Section 2.2.

1. 126: Edgar > EDGAR

   Done!

2. 128: finn > FINN?

   Done!

3. How come the wetland prior map is so weak in Pakistan, while 10% of Pakistan's land is wetlands? Maybe use proper scales for each panel? Use non-linear scales for flux maps, as you will miss some key information.

   This is not a matter of the flux scales. The wetland emissions in Pakistan are indeed very low (1 order less or even lower than in other places) in the prior inventories and do not appear in large scale as for Bangladesh. The bottom-up inventories estimate an emission of only **< 0.1 Tg/yr** of wetland emissions from Pakistan. In the recent study on wetland emissions by Chen et al., 2025, you can see the spatial distribution of wetland emissions as similar to our map.

4. 146: Significant landfill emissions can also be in other major cities. Maybe elaborate on other regions also.

   Notably high landfill emissions can also be found over the capital city of India, Delhi

   Changed to:

   "Notably regions of high landfill emissions can also be found over Islamabad, Delhi, Mumbai, Ahmedabad and Bangalore (Dogniaux et al., 2025; Toha et al., 2025)"

5. Table 1. Edgar > "EDGAR"

   Done!

Section 2.3.

1. Include reference to CAMS, EGG4, etc.

   Done!

2. ECMWF- write in full at the first use for all abbreviations (e.g. RMSD in line 166)

   Done!

Section 2.4

1. 169: Flexpart > FLEXPART

   Done!

Results

1. The prior map clearly shows emissions from anthropogenic sources in the LIB. So, how do the river discharge peaks correspond to methane emissions? If it is related to rain-fed agriculture, this should be clearly written with some references. (What is the agricultural practice in Pakistan etc.). Wetlands in Pakistan are also in the region where you have anthropogenic emissions (your wetland prior plot does not show that due to large emissions from Bangladesh). So the double peak, is it from seasonally inundated wetlands or seasonal agriculture?

   Both mechanisms are plausible. The inversion cannot tell us which mechanism is driving the emissions. We believe that the emissions are often due to the combination of both agricultural practices and wetland inundation, since both depend on precipitation and run-off. The emission peak in May could be driven by increased river-flow from snow melt and due to the onset of irrigated rice cultivation and the August peak with monsoon-driven inundation.

   There are basically two main agricultural seasons for Pakistan: Kharif and Rabi Seasons. Kharif crops require a lot of water to grow. For Kharif season, seeds are sowed from April-June and harvested at the end of the monsoon. So, this could lead to emission in April-June. The second peak could be partly due to the monsoon driven inundation and partly from the agricultural conditions. No studies directly address the seasonal features of Pakistan's wetland inundation and agricultural practices.

2. Also, the aggregated posterior for SA also shows peaks in two seasons, as has been shown in some previous studies (e.g., Ganesan et al., 2017) for Indian agriculture emissions. So emphasis may be given to the whole domain instead of LIB.

   We agree that the aggregated posterior emissions over South Asia show clear seasonal peaks and that this domain-wide perspective is important. At the same time, we show the sub regional analyses because the processes driving methane seasonality differ across South Asia. Investigating subregions helps to interpret the underlying mechanisms. For example, the Lower Indus Basin (LIB) exhibits a seasonal pattern influenced partly by snowmelt-driven river discharge (Baig et al., 2022), whereas Bangladesh shows a stronger direct response to monsoon-driven inundation. The presence of physically consistent but distinct seasonal behavior across these regions supports the credibility of the inferred emission patterns.

3. Should mention in the Figure 10 caption about the prior uncertainty? How is the prior uncertainty calculated? Is it not small for South Asia?

   The prior inventories do not specify uncertainties. We have assumed them to be 100% of the prior fluxes on a grid cell level but with a lower limit of 1×10^{-9} kg m^{-2} h^{-1} ($2.8\text{x}10^{-13}$ kg m^{-2} s^{-1}). Prior error correlations are represented using an exponential decay function with a spatial correlation length of 250 km and a temporal scale of 30 days. The aggregated uncertainties are calculated as the root sum square of individual uncertainties. In the earlier calculations, the error cross-correlations were not considered when deriving uncertainties. Now we have included this, which leads to more realistic prior (66.3 ± 6.7 Tg yr^{-1}) and posterior uncertainty (73 ± 0.7 Tg yr^{-1}) estimates over South Asia. The smaller posterior uncertainty reflects the stronger constraint provided by the TROPOMI observations through the inverse calculation.

4. “However, since this validation is not against independent data, this shows only that the inversion is performing as expected”. A posterior simulation with independent surface observation should be done, as satellite data are not real observations. So, make use of surface observations to demonstrate that the posterior fits well with observations in this region.

   In the absence of suitable surface observations, we validated the posterior simulation against the independent GOSAT–TROPOMI blended XCH_4 dataset (Balasus et al., 2023), which is developed independently of the WFMD retrievals used in this study.

5. Figure 11 gives the ensemble values, but where does it stand when compared to prior or recent studies? More information can be added there. Also, provide prior/posterior uncertainty in all applicable figures (e.g., no prior uncertainty in Figure 12, no posterior uncertainty in Figure 11).

   Prior estimate is 66.3 Tg ± 6.7 Tg yr^{-1}. We have now added the prior value in the figure 11 for easier comparison. Estimates from the recent studies were shown earlier in the introduction part as figure 1. Now we have moved this figure to the results part so that it is clear where our estimates stand compared to other studies.

   Thanks for pointing this out. Uncertainties are added to the figures. In figure 12, posterior ensemble standard deviation is shown with error bar, since prior flux is not perturbed here, there is no spread in prior values hence the error bar is not drawn there. Now, the prescribed prior uncertainty for the reference inversion is added as the error bar for prior fluxes.

6. Figure 12. Group the regions together (darker/lighter) for direct comparison to the respective prior.

   Thanks for the comment, we have now modified the figure.

7. 267-269: "The model prior mole fractions (orange line) significantly overestimate". No need for ‘(orange line)’ etc in the text.

Removed!

8. 295-296: "Figure 8 (c) shows the spatial distribution of the increments in the methane fluxes after the inversion (posterior-prior)". The word 'increment' normally implies a positive addition. Maybe better to refer to it as flux correction or adjustments

   Flux increments changed to flux correction.

9. 302 "trajectory of the river Yamuna and Ganges,". Trajectory may be replaced by 'course' or something more appropriate.

   Trajectory changed to course.

10. 303-305 "Several studies have shown rice cultivation as a key contributor to methane emissions here due to the use of nitrogen fertilizers, organic manure, and livestock population in this region [Singh et al., 2021]". Be generous with citations when you say 'several'.

    Several studies have shown rice cultivation as a key contributor to methane emissions here due to the use of nitrogen fertilizers, organic manure, and livestock population in this region [Singh et al., 2021].

    Changed to:

    Several studies have shown rice cultivation as a key contributor to methane emissions here (Anand et al., 2005; Gupta et al., 2015; Manjunath et al., 2006; Matthews et al., 1991) due to the use of nitrogen fertilizers, organic manure, and livestock population in this region (Singh et al., 2021)

11. 307-308 'In the area marked within the blue box,'. You should not be writing about the marked boxes, but specifically write Upper Indus Basin or whatever you can geographically name it

    In the area marked within the blue box, emission estimates are reduced by -2.4 Tg yr^{-1}

    Changed to:

    In the Upper Indus Basin (blue box), emission estimates are reduced by -2.4 Tg yr^{-1}

Conclusion

1. 419-420 "…the back box region…". This is not an appropriate reference to the analysis region in conclusion. Specify the region so that the conclusion stands alone.

   Within this increase, Bangladesh alone contributes +5.6 Tg yr-1, while the black-box region covering eastern India and Bangladesh accounts for +8.4 Tg yr^{-1} of the regional increment.

   Changed to:

   Within this increase, Bangladesh alone contributes +5.6 Tg yr-1, while the region covering eastern India and Bangladesh (black box) accounts for +8.4 Tg yr^{-1} of the regional increment.

2. "These analyses suggest that the 2020 rise in methane emissions is strongly linked to biogenic processes driven by glacial melt (in the Indus river basin), heavy monsoonal rainfall and enhanced inundation (both in the Indus river basin and in Bangladesh). These findings are consistent with earlier studies (e.g., Peng et al., (2022), Niwa et al., (2025)) that identify wetlands and agriculture

as dominant contributors to the regional and global methane budget in recent years.” Since you estimate only one year of emission, you do not need to tell from this particular study that there was a rise in 2020.

Removed “2020”

References

Anand, S., Dahiya, R. P., Talyan, V., and Vrat, P.: Investigations of methane emissions from rice cultivation in Indian context, Environment International, 31, 469–482, https://doi.org/10.1016/j.envint.2004.10.016, 2005.

Baig, S., Sayama, T., and Yamada, M.: Quantifying the changes in the runoff and its components across the Upper Indus River Basin under climate change, Journal of Water and Climate Change, 13, 3416–3434, https://doi.org/10.2166/wcc.2022.153, 2022.

Balasus, N., Jacob, D. J., Lorente, A., Maasakkers, J. D., Parker, R. J., Boesch, H., Chen, Z., Kelp, M. M., Nesser, H., and Varon, D. J.: A blended TROPOMI+GOSAT satellite data product for atmospheric methane using machine learning to correct retrieval biases, Atmospheric Measurement Techniques, 16, 3787–3807, https://doi.org/10.5194/amt-16-3787-2023, 2023.

Bovensmann, H., Burrows, J. P., Buchwitz, M., Frerick, J., Noël, S., Rozanov, V. V., Chance, K. V., and Goede, A. P. H.: SCIAMACHY: Mission Objectives and Measurement Modes, Journal of the Atmospheric Sciences, 56, 127–150, https://doi.org/10.1175/1520-0469(1999)056%253C0127:SMOAMM%253E2.0.CO;2, 1999.

Chandra, N., Patra, P. K., Bisht, J. S. H., Ito, A., Umezawa, T., Saigusa, N., Morimoto, S., Aoki, S., Janssens-Maenhout, G., Fujita, R., Takigawa, M., Watanabe, S., Saitoh, N., and Canadell, J. G.: Emissions from the Oil and Gas Sectors, Coal Mining and Ruminant Farming Drive Methane Growth over the Past Three Decades, Journal of the Meteorological Society of Japan. Ser. II, 99, 309–337, https://doi.org/10.2151/jmsj.2021-015, 2021.

Chen, A., Zhang, Z., Poulter, B., Feng, L., Liu, H., Murray, L. T., Yu, X., Huang, Z., Gaeta, D. C., Morgan, K. L., Zhu, Q., and Miller, S. M.: Spatial and Temporal Distribution of Global Wetland Methane Emissions During 2019–2020 Estimated From Satellite Observations, Journal of Geophysical Research: Atmospheres, 130, e2025JD044354, https://doi.org/10.1029/2025JD044354, 2025.

Dogniaux, M., Maasakkers, J. D., Girard, M., Jervis, D., McKeever, J., Schuit, B. J., Sharma, S., Lopez-Noreña, A., Varon, D. J., and Aben, I.: Global satellite survey reveals uncertainty in landfill methane emissions, Nature, 647, 397–402, https://doi.org/10.1038/s41586-025-09683-8, 2025.

Ganesan, A. L., Rigby, M., Lunt, M. F., Parker, R. J., Boesch, H., Goulding, N., Umezawa, T., Zahn, A., Chatterjee, A., Prinn, R. G., Tiwari, Y. K., Van Der Schoot, M., and Krummel, P. B.: Atmospheric observations show accurate reporting and little growth in India’s methane emissions, Nat Commun, 8, 836, https://doi.org/10.1038/s41467-017-00994-7, 2017.

Gupta, D. K., Bhatia, A., Kumar, A., Chakrabarti, B., Jain, N., and Pathak, H.: Global warming potential of rice (Oryza sativa)-wheat (Triticum aestivum) cropping system of the Indo-Gangetic Plains, Indian J Agri Sci, 85, 807–816, https://doi.org/10.56093/ijas.v85i6.49243, 2015.

Hu, H., Hasekamp, O., Butz, A., Galli, A., Landgraf, J., Aan de Brugh, J., Borsdorff, T., Scheepmaker, R., and Aben, I.: The operational methane retrieval algorithm for TROPOMI, Atmospheric Measurement Techniques, 9, 5423–5440, https://doi.org/10.5194/amt-9-5423-2016, 2016.

International Energy Agency: Methane and climate change – Methane Tracker 2021, https://www.iea.org/reports/methane-tracker-2021/methane-and-climate-change, 2021.

Jacob, D. J., Varon, D. J., Cusworth, D. H., Dennison, P. E., Frankenberg, C., Gautam, R., Guanter, L., Kelley, J., McKeever, J., Ott, L. E., Poulter, B., Qu, Z., Thorpe, A. K., Worden, J. R., and Duren, R. M.: Quantifying methane emissions from the global scale down to point sources using satellite observations of atmospheric methane, Atmospheric Chemistry and Physics, 22, 9617–9646, https://doi.org/10.5194/acp-22-9617-2022, 2022.

Janardanan, R., Maksyutov, S., Tsuruta, A., Wang, F., Tiwari, Y. K., Valsala, V., Ito, A., Yoshida, Y., Kaiser, J. W., Janssens-Maenhout, G., Arshinov, M., Sasakawa, M., Tohjima, Y., Worthy, D. E. J., Dlugokencky, E. J., Ramonet, M., Arduini, J., Lavric, J. V., Piacentino, S., Krummel, P. B., Langenfelds, R. L., Mammarella, I., and Matsunaga, T.: Country-Scale Analysis of Methane Emissions with a High-Resolution Inverse Model Using GOSAT and Surface Observations, Remote Sensing, 12, 375, https://doi.org/10.3390/rs12030375, 2020.

Jones, A., Thomson, D., Hort, M., and Devenish, B.: The U.K. Met Office's Next-Generation Atmospheric Dispersion Model, NAME III, in: Air Pollution Modeling and Its Application XVII, 580–589, https://doi.org/10.1007/978-0-387-68854-1_62, 2007.

Jongaramrungruang, S., Matheou, G., Thorpe, A. K., Zeng, Z.-C., and Frankenberg, C.: Remote sensing of methane plumes: instrument tradeoff analysis for detecting and quantifying local sources at global scale, Atmospheric Measurement Techniques, 14, 7999–8017, https://doi.org/10.5194/amt-14-7999-2021, 2021.

Kuze, A., Suto, H., Nakajima, M., and Hamazaki, T.: Thermal and near infrared sensor for carbon observation Fourier-transform spectrometer on the Greenhouse Gases Observing Satellite for greenhouse gases monitoring, Appl. Opt., AO, 48, 6716–6733, https://doi.org/10.1364/AO.48.006716, 2009.

Kuze, A., Kikuchi, N., Kataoka, F., Suto, H., Shiomi, K., and Kondo, Y.: Detection of Methane Emission from a Local Source Using GOSAT Target Observations, Remote Sensing, 12, 267, https://doi.org/10.3390/rs12020267, 2020.

Lama, S., Maasakkers, J. D., Zhang, X., Girard, M., Dutt, S., Nandgaonkar, S., Varon, D. J., Sulprizio, M. P., Estrada, L. A., Balasus, N., Parker, R. J., Terao, Y., and Aben, I.: Evaluating national, state, and urban Indian methane emissions using satellites, EGUsphere, 1–36, https://doi.org/10.5194/egusphere-2025-6528, 2026.

Li, M., Kort, E. A., Bloom, A. A., Wu, D., Plant, G., Gerlein-Safdi, C., and Pu, T.: Underestimated Dry Season Methane Emissions from Wetlands in the Pantanal, Environ. Sci. Technol., 58, 3278–3287, https://doi.org/10.1021/acs.est.3c09250, 2024.

Liang, R., Zhang, Y., Chen, W., Zhang, P., Liu, J., Chen, C., Mao, H., Shen, G., Qu, Z., Chen, Z., Zhou, M., Wang, P., Parker, R. J., Boesch, H., Lorente, A., Maasakkers, J. D., and Aben, I.: East Asian methane emissions inferred from high-resolution inversions of GOSAT and TROPOMI observations: a comparative and evaluative analysis, Atmospheric Chemistry and Physics, 23, 8039–8057, https://doi.org/10.5194/acp-23-8039-2023, 2023.

Lindqvist, H., Kivimäki, E., Häkkilä, T., Tsuruta, A., Schneising, O., Buchwitz, M., Lorente, A., Martinez Velarte, M., Borsdorff, T., Alberti, C., Backman, L., Buschmann, M., Chen, H., Dubravica, D., Hase, F., Heikkinen, P., Karppinen, T., Kivi, R., McGee, E., Notholt, J., Rautiainen, K., Roche, S., Simpson, W., Strong, K., Tu, Q., Wunch, D., Aalto, T., and Tamminen, J.: Evaluation of Sentinel-5P TROPOMI Methane Observations at Northern High Latitudes, Remote Sensing, 16, 2979, https://doi.org/10.3390/rs16162979, 2024.

Lorente, A., Borsdorff, T., Butz, A., Hasekamp, O., aan de Brugh, J., Schneider, A., Wu, L., Hase, F., Kivi, R., Wunch, D., Pollard, D. F., Shiomi, K., Deutscher, N. M., Velazco, V. A., Roehl, C. M., Wennberg, P. O., Warneke, T., and Landgraf, J.: Methane retrieved from TROPOMI: improvement of the data product and validation of the first 2 years of measurements, Atmospheric Measurement Techniques, 14, 665–684, https://doi.org/10.5194/amt-14-665-2021, 2021.

Lorente, A., Borsdorff, T., Martinez-Velarte, M. C., and Landgraf, J.: Accounting for surface reflectance spectral features in TROPOMI methane retrievals, Atmos. Meas. Tech., 16, 1597–1608, https://doi.org/10.5194/amt-16-1597-2023, 2023.

Manjunath, K. R., Panigrahy, S., Kumari, K., Adhya, T. K., and Parihar, J. S.: Spatiotemporal modelling of methane flux from the rice fields of India using remote sensing and GIS, International Journal of Remote Sensing, 27, 4701–4707, https://doi.org/10.1080/01431160600702350, 2006.

Matthews, E., Fung, I., and Lerner, J.: Methane emission from rice cultivation: Geographic and seasonal distribution of cultivated areas and emissions, Global Biogeochemical Cycles, 5, 3–24, https://doi.org/10.1029/90GB02311, 1991.

Miller, S. M., Michalak, A. M., Detmers, R. G., Hasekamp, O. P., Bruhwiler, L. M. P., and Schwietzke, S.: China's coal mine methane regulations have not curbed growing emissions, Nat Commun, 10, 303, https://doi.org/10.1038/s41467-018-07891-7, 2019.

Schneising, O., Buchwitz, M., Hachmeister, J., Vanselow, S., Reuter, M., Buschmann, M., Bovensmann, H., and Burrows, J. P.: Advances in retrieving XCH_4 and XCO from Sentinel-5 Precursor: improvements in the scientific TROPOMI/WFMD algorithm, Atmospheric Measurement Techniques, 16, 669–694, https://doi.org/10.5194/amt-16-669-2023, 2023.

Singh, A., Kuttippurath, J., Abbhishek, K., Mallick, N., Raj, S., Chander, G., and Dixit, S.: Biogenic link to the recent increase in atmospheric methane over India, Journal of Environmental Management, 289, 112526, https://doi.org/10.1016/j.jenvman.2021.112526, 2021.

Thompson, R. L., Krishnankutty, N., Pisso, I., Schneider, P., Stebel, K., Sasakawa, M., Stohl, A., and Platt, S. M.: Efficient use of a Lagrangian particle dispersion model for atmospheric inversions using satellite observations of column mixing ratios, Atmospheric Chemistry and Physics, 25, 12737–12751, https://doi.org/10.5194/acp-25-12737-2025, 2025.

Toha, M., Ariyan, T. N., and Alam, M.: Methane hotspots in landfills: A systematic review on transboundary dispersion and impacts on heatwaves in South Asia, Cleaner Waste Systems, 10, 100235, https://doi.org/10.1016/j.clwas.2025.100235, 2025.

Worden, J. R., Cusworth, D. H., Qu, Z., Yin, Y., Zhang, Y., Bloom, A. A., Ma, S., Byrne, B. K., Scarpelli, T., Maasakkers, J. D., Crisp, D., Duren, R., and Jacob, D. J.: The 2019 methane budget and uncertainties at 1° resolution and each country through Bayesian integration Of GOSAT total column methane data and a priori inventory estimates, Atmospheric Chemistry and Physics, 22, 6811–6841, https://doi.org/10.5194/acp-22-6811-2022, 2022.

Wu, D., Lin, J. C., Fasoli, B., Oda, T., Ye, X., Lauvaux, T., Yang, E. G., and Kort, E. A.: A Lagrangian approach towards extracting signals of urban CO_2 emissions from satellite observations of atmospheric column CO_2 (XCO_2): X-Stochastic Time-Inverted Lagrangian Transport model ("X-STILT v1"), Geoscientific Model Development, 11, 4843–4871, https://doi.org/10.5194/gmd-11-4843-2018, 2018.

Yu, X., Millet, D. B., Henze, D. K., Turner, A. J., Delgado, A. L., Bloom, A. A., and Sheng, J.: A high-resolution satellite-based map of global methane emissions reveals missing wetland, fossil fuel, and monsoon sources, Atmospheric Chemistry and Physics, 23, 3325–3346, https://doi.org/10.5194/acp-23-3325-2023, 2023.

Reviewer #2 Comments:

We thank the reviewer for the important and constructive comments. In the following, we repeat the reviewer's comments in black and insert our answers in blue. In some cases, we highlight the changes made in the manuscript, written in italic font whereas the original text is repeated with grey coloring.

Review of 'Strong monsoon influence on South Asian methane emissions in 2020 revealed by a Bayesian inversion constrained by satellite observations"

Anita Ganesan

The authors present a new study using TROPOMI observations from 2020 to quantify methane emissions from South Asia. The authors employ the FLEXPART and FLEXINVERT methodologies. The manuscript is well-written, and it is well-worth using TROPOMI data to try to quantify emissions from this important region.

However, I have two major reservations: First is that many interpretations are based on correlations of monthly fluxes and other data using one year of data (i.e. correlating 12 monthly fluxes with 12 monthly average rainfall, etc data). Large sections are thus quite speculative because there just isn't a long enough timeseries of results to do this kind of analysis. My recommendation would be to remove the speculative results (they can still be mentioned in the context of discussion and future work when longer inversion results can be derived).

We agree with the reviewer that one year of inversion results may not be sufficient to support robust statistical inference based on correlations of monthly mean quantities. Our intention was to explore whether the posterior flux variability indicates patterns that are consistent with hydrological variability during an anomalous monsoon year. Following the reviewer's recommendation, we will revise the manuscript to frame all correlation-based analyses as exploratory and state that establishing a strong relationship between flux and hydrology requires multi-year inversion results, which are beyond the scope of the present study but constitute an important direction for future work.

To evaluate whether our results only reflect the conditions for the year 2020, we conducted an additional FLEXPART simulation for 2019 using the same model configuration, but at a coarser temporal resolution. Here the transport simulations are done only for once in every 5 days and the prior model and background methane mole fractions calculated at 5-day intervals. For calculating this, we used the same prior and background field datasets but for the year 2019. The corresponding time series is shown in the Figure S1.

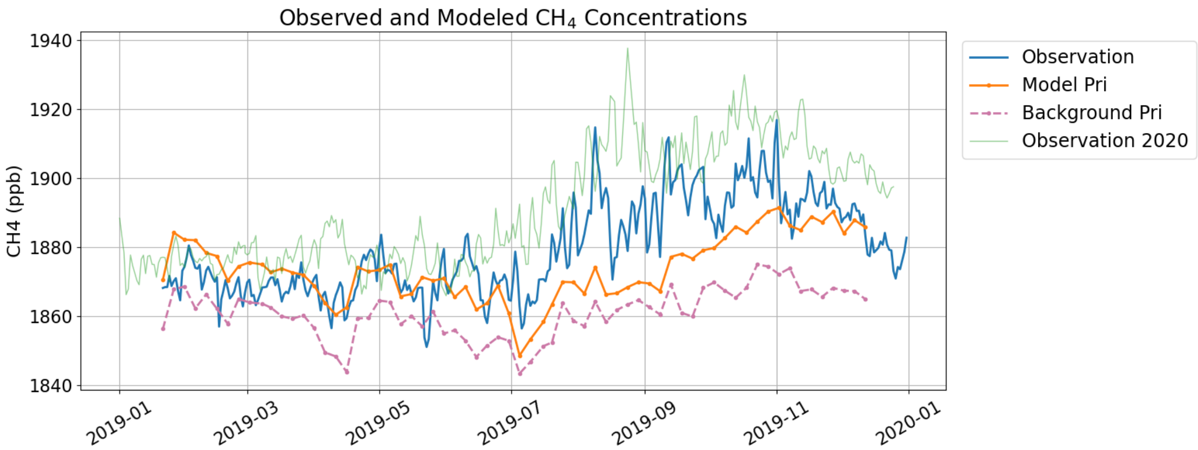

Figure S1. Time series of observed and modeled prior methane (CH_4) column-averaged dry air mole fractions averaged over South Asia for the year 2019.

The 2019 prior concentration time series indicate a seasonality comparable to that of 2020, including relative overestimation by the model using prior emissions during Jan-May and underestimation during Jun-Sep. This consistency suggests that the seasonal signal is not unique to a single year. Furthermore, regional inversion studies using TROPOMI observations over East Asia (e.g., Liang et al., 2023) report spatial increment patterns for 2019 consistent with the type of monsoon-related variability identified in our analysis. However, as the 2019 experiment was conducted at reduced temporal resolution and does not constitute an inversion analysis, we present this comparison as qualitative support rather than quantitative validation.

We agree, however, that a rigorous statistical assessment of flux–hydrology relationships requires a multi-year inversion framework. Such an analysis is beyond the scope of the present study but represents an important direction for future work. We will clarify this limitation in the revised manuscript.

Second, the manuscript also requires a more comprehensive evaluation on the use of satellite data for national-scale emissions estimation, which currently is still debated. As this is a topic of interest to the community, the manuscript should do more to convince that satellite-derived estimates are robust (or not). Even if the result is that they are not robust (i.e., they are sensitive to many assumptions which we see documented in other studies), that is still a valuable contribution to the community and helps the community learn more about this growing field.

We thank the reviewer for this point. The robustness of satellite constrained national scale emission estimates is an active and ongoing discussion in the community and we agree that this aspect deserves careful consideration. Several previous studies have successfully used satellite observations to estimate methane emissions at national and regional scales (Janardanan et al., 2020; Lama et al., 2026; Miller et al., 2019; Worden et al., 2022; Yu et al., 2023). These studies demonstrate that satellite-based inversions can provide meaningful constraints. We summarize their regional methane budget estimates in the introduction section to place our results in context.

However, in the particular case of South Asia, unfortunately, it is not trivial to validate the inversion results, since ground-based observations are not available (or accessible to us) at all for this region. To address the robustness of our satellite constrained estimates, we have strengthened the manuscript in the following ways:

1. Sensitivity to Prior Flux Magnitude
   We scaled the prior emission inventory to 50%, 80%, 120%, and 200% of its original magnitude and test whether the inversion captures the same spatial and seasonal patterns. The result of this is shown as the response to the major comments 2.
2. Independent Column Evaluation
   In the absence of suitable representative ground-based data, we have now used the GOSAT-TROPOMI Blended retrieval product by Balasus et al., 2023 to evaluate prior and posterior modeled columns. This provides a partly independent assessment of modeled column behavior. The analysis with this data is provided at the end of this document and will be added to the revised manuscript.

Together these analyses indicate that the satellite observations provide meaningful constraint on methane emissions at the national scale for South Asia in 2020.

I have added my name to this review in case it is helpful to you to discuss/clarify any of the comments. Major

comments:

1) Discussion with past work – I was surprised that there was little discussion or comparison with previous work, particularly our study Ganesan et al 2017 which used this same technique (Lagrangian SRRs) but with a different dataset GOSAT and model (NAME). What would be useful to the community is in understanding if and why satellite datasets produce different results. The use of satellite data for national-scale emissions estimation has been proposed as a way forward for many countries and this paper could be used to add to that discussion. I would like to see more of this discussion made and a critical evaluation presented.

We thank the reviewer for highlighting the close methodological link to Ganesan et al., 2017. We have now expanded the introduction section to compare our approach with this earlier Lagrangian SRR-based satellite inversion, clarifying both the methodological similarities and the key extensions enabled by the use of TROPOMI observations and a different inversion framework.

Differences between satellite and surface-based inversions can arise from the fundamentally different spatial sampling characteristics of the observations. Several recent studies using satellite observations (e.g., (Janardanan et al., 2020; Miller et al., 2019; Worden et al., 2022; Yu et al., 2023) report higher national methane emission estimates compared to earlier surface-based inversions, which may reflect improved constraints in previously under-sampled regions. With respect to the comparison between Ganesan et al. (2017) and the present study, it is important to distinguish between differences arising from retrieval characteristics, coverage and frequency of the data and from the actual atmospheric state. Ganesan et al. (2017) analyzed the period 2010–2015, when the emissions in India were likely substantially different from the year 2020, given the rapid population growth and industrial development during this decade. Differences between the two studies are therefore expected. Indeed, studies such as Chandra et al., 2021 and Miller et al., 2019 have similarly noted that emissions for India have substantially increased since then. This suggests that the difference may indeed reflect genuine emission increases in recent years, in addition to the improved constraint from the more frequent TROPOMI observations compared to GOSAT data.

We have now added the comparison with previous works, Ganesan et al., 2017 and discussed about the differences.

2) The sensitivity analysis is fairly limited (looking at changing uncertainty sizes) in Section 3.2. An important consideration would be sensitivity to the prior flux magnitude itself, not just the level of random uncertainty. Given the lower signal to noise of column data over point data, it is possible that the prior flux magnitude influences the results and this should be an important factor examined. What if the prior fluxes were twice or half as large? The posterior fluxes are largely the same as prior fluxes, which doesn't necessarily mean it is due to the prior, but still should be checked. Other studies on TROPOMI inversions have also shown that the two retrievals (operational and WMFD) also lead to different results – this is not investigated – but also is important in the context of understanding the state-of-play in this field.

We thank the reviewer for the suggestion. Following this recommendation, we have performed an additional sensitivity analysis examining the impact of prior flux magnitude on the inversion results. We scaled the total prior emissions to 50%, 80%, 120%, and 200% of the reference prior while keeping all other inversion settings unchanged. This corresponds to a wide range of prior flux magnitudes (~33–133 Tg CH_4 yr^{-1}). The results are presented here in Figure S2 and S3. The corresponding posterior total emissions are 65.7, 70.6, 71.4, and 71.7 Tg yr^{-1} for the 50%, 80%, 120%, and 200% prior cases, respectively, compared to 73 Tg yr^{-1} in the reference inversion. Despite large changes in prior magnitude, the posterior fluxes converge toward a relatively narrow range, indicating that the inversion is not strongly controlled by the prior magnitude. The spatial increment patterns are also qualitatively consistent across the ensemble members (Figure S3). These results suggest that the posterior solution is primarily constrained by the observational information rather than being dominated by the prior flux magnitude, even under substantial perturbations. We will add a discussion of this sensitivity test in the manuscript.

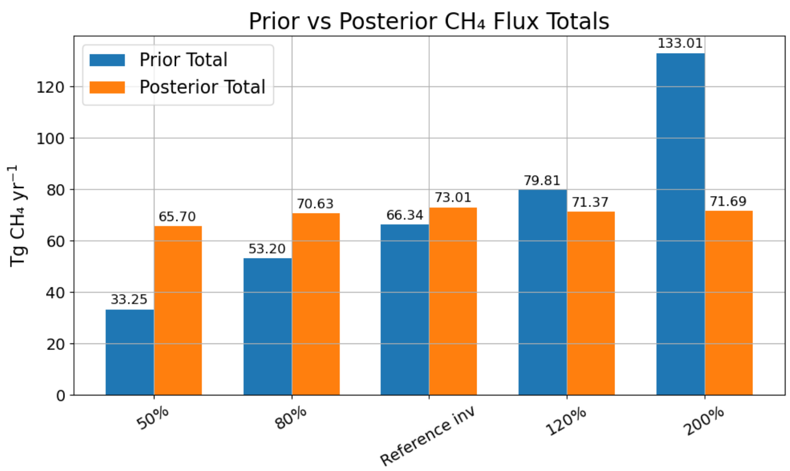

Figure S2. Sensitivity of total posterior methane emissions to prior flux magnitude scaling. The prior inventory was uniformly scaled to 50%, 80%, 120%, and 200% of its original magnitude. Blue bars show the corresponding prior totals and orange bars the posterior totals.

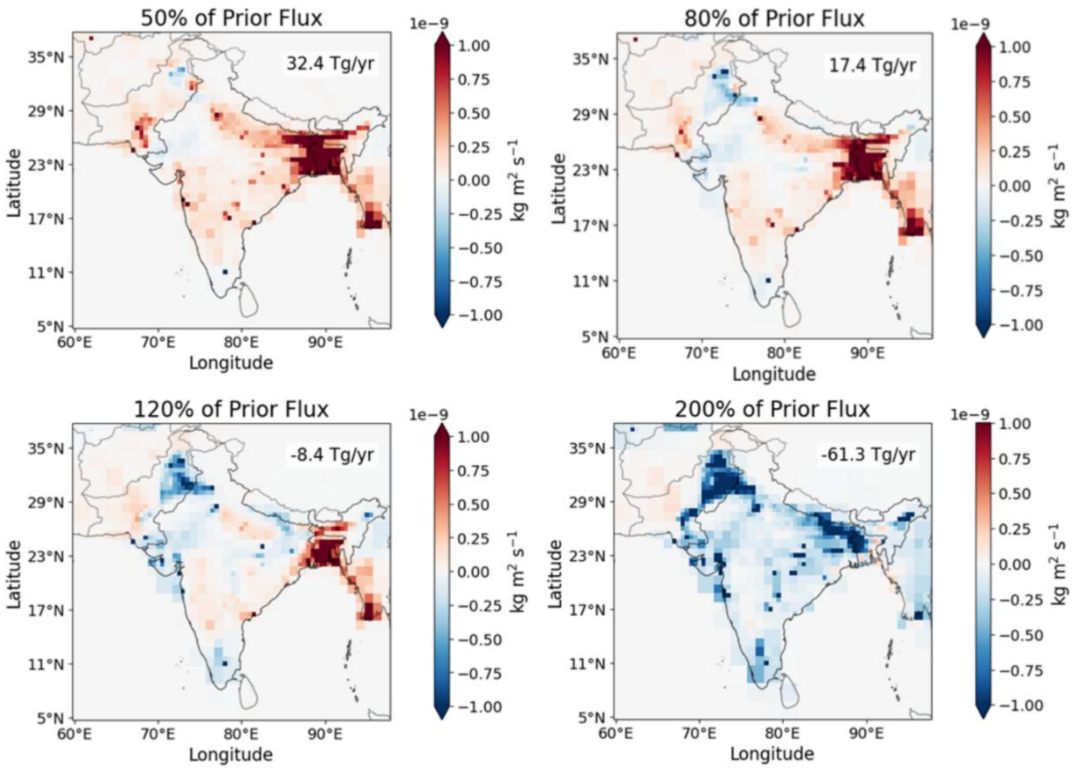

Figure S3. Spatial distribution of posterior flux increments (posterior minus prior; kg m^{-2} s^{-1}) over South Asia for sensitivity experiments in which the prior flux magnitude was uniformly scaled to 50%, 80%, 120%, and 200% of the reference inventory. The numbers shown in each panel indicate the corresponding total flux increment (Tg CH_4 yr^{-1}). Positive values (red) denote regions where posterior emissions exceed the prior, while negative values (blue) indicate downward adjustments. Although the magnitude and sign of total increments vary with prior scaling, the principal spatial adjustment patterns, particularly over eastern India, Bangladesh, and parts of the Indus basin remain qualitatively consistent across experiments, indicating limited sensitivity of spatial correction structures to the assumed prior magnitude.

With respect to the sensitivity to different TROPOMI retrieval products (e.g., operational versus WFMD), we agree that retrieval dependent differences are an important consideration. In this study, we focused on the WFMD product due to its documented albedo corrections, destriping and bias correction characteristics. Then we use the GOSAT-TROPOMI blended product for validation, which is developed independently of the WFMD TROPOMI retrievals used in our inversion. A systematic intercomparison of retrieval products would require a dedicated set of additional inversions and is beyond the scope of the present work. We will clarify this limitation in the revised manuscript and note it as an important direction for future investigation.

3) Time period – why is the analysis only performed for one year – 2020 – given that there is not several more years of data available? Even additional year or two would help to understand whether the patterns are robust (as the monsoon is an annual feature). If not possible, then it is important to stress up front that this only reflects one year of analysis and therefore change the results presented (see next point).

We agree that extending the analysis to multiple years would be valuable. Due to the computational constraints we presented here the forward runs at a coarser resolution for the year 2019. Even though this experiment shows similar results as for the year 2020, in the revised manuscript, we will state that the study only reflects one year of analysis.

4) Given the flux estimates for only one year (i.e., 12 monthly fluxes), the analyses of runoff in UIB/LIB and correlation of fluxes with rainfall seems very speculative (also given the uncertainties in the runoff data, the influence on irrigation in correlating moisture with emissions). It is a stretch to do this type of analysis with such a short record as the statistics will be very uncertain. A way forward could be that these analyses are removed and the paper rather extended on how robust national and sub-national inversion estimates from satellite data are over South Asia. These analyses on drivers could then still be mentioned in Discussion as a valuable extension with

more years of results.

We agree that statistical inference based on 12 monthly values is limited. We therefore consider this more as a case study, where our intention was to examine whether the posterior seasonal flux seasonality is physically consistent with large-scale hydrological variability during the study year. To evaluate whether the hydrological patterns observed in 2020 were anomalous, we have examined the corresponding rainfall, runoff, and soil wetness fields for 2019. The 2019 runoff evolution in both the Upper and Lower Indus Basins reveals a similar seasonal progression (Figure S4), with monsoon-driven peaks during mid-year. Likewise, the domain averaged rainfall, runoff, and soil wetness over South Asia and the Bangladesh region display a comparable seasonal structure in 2019 (Figure S5), indicating that the hydrological cycle reflected in our analysis is climatologically consistent rather than specific to 2020.

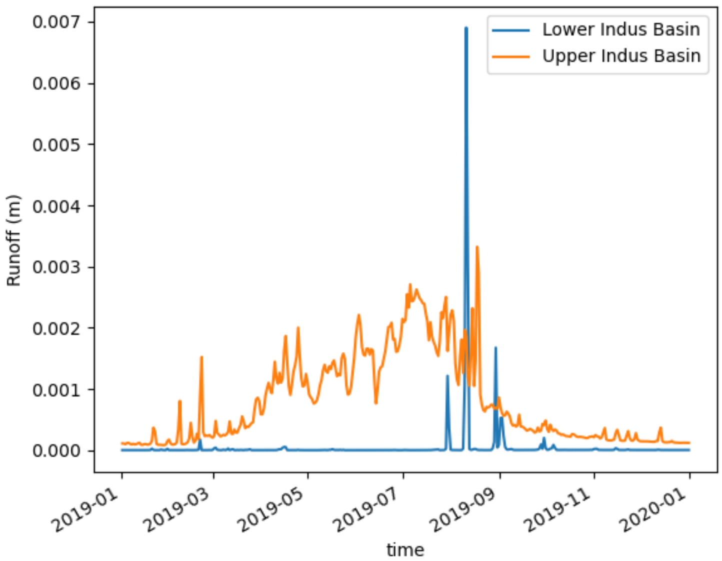

Figure S4. Runoff time series (m) for the Upper Indus Basin (orange) and Lower Indus Basin (blue) for the year 2019.

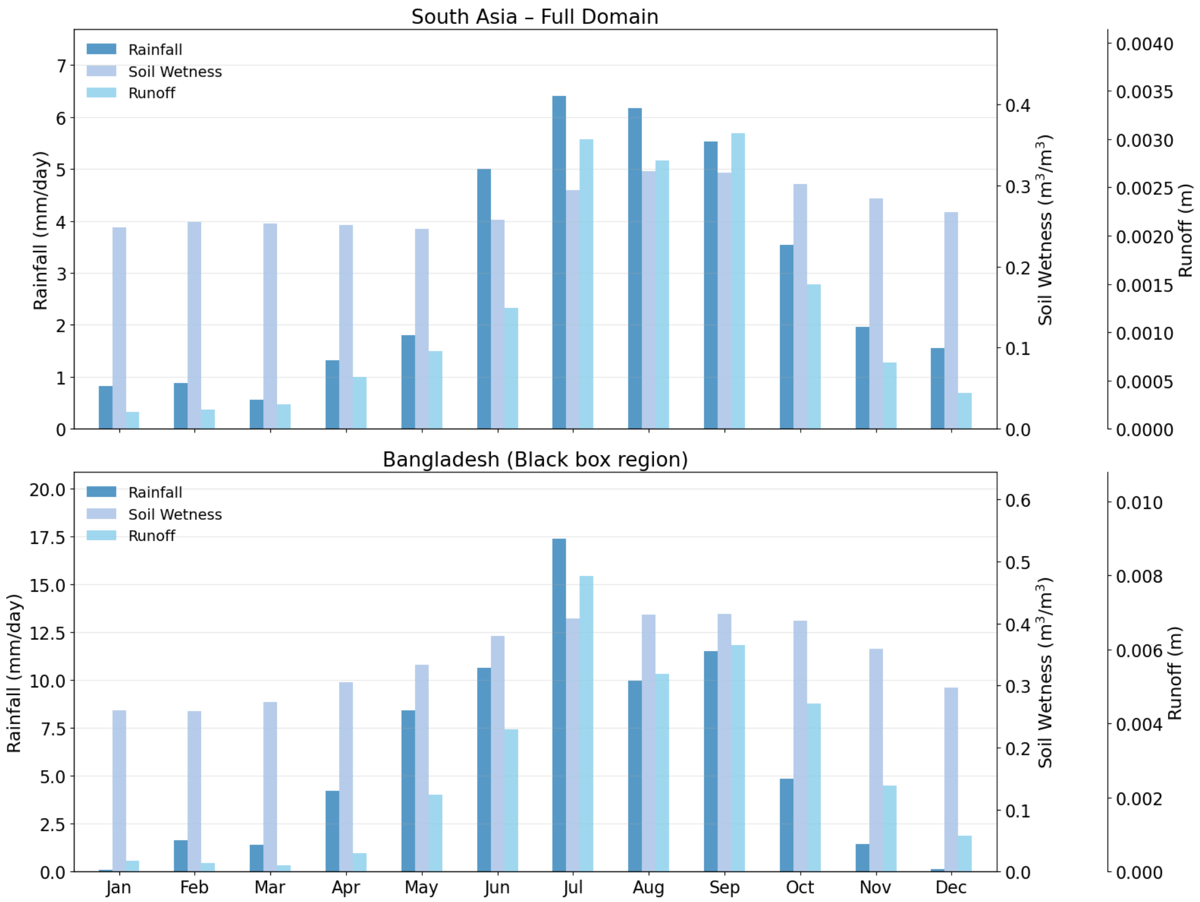

Figure S5. Monthly rainfall, soil wetness, and runoff over South Asia and the Bangladesh (black box) region for the year 2019. Top panel: across the full South Asian study region. Bottom panel: for the Bangladesh (black box) region. Both panels show a clear seasonal cycle characterized by enhanced rainfall, soil wetness, and runoff during the monsoon months (Jun–Sep), with reduced values during the dry season.

With respect to robustness, we note that the stability of the inversion results has been evaluated independently through additional sensitivity tests and validation analyses.

5) The impact of the background is not discussed in much detail – during the July – Nov period, the background drops significantly lower than the observations, implying that the background is only being indirectly constrained (i.e. there are no observations that are representative of background conditions). Furthermore, boundary conditions could alias with emissions, particularly over such a small domain. The posterior background is higher in August than January suggesting regional emissions impact the background. How sensitive are the derived results to different assumptions about the background? If different boundary conditions were used, what is the impact? The text states CAMS was also used – but I don't see those results presented. All of this needs some discussion.

We agree that the role of the background concentration field is critical, particularly given the relatively small size of the inversion domain and the potential for boundary-condition aliasing with surface emissions.

Since the Figure 7 in the manuscript is a mean picture, the finer details were not clearly visible. Now we plotted the observed and the modeled background mole fractions for Jul-Nov without averaging.

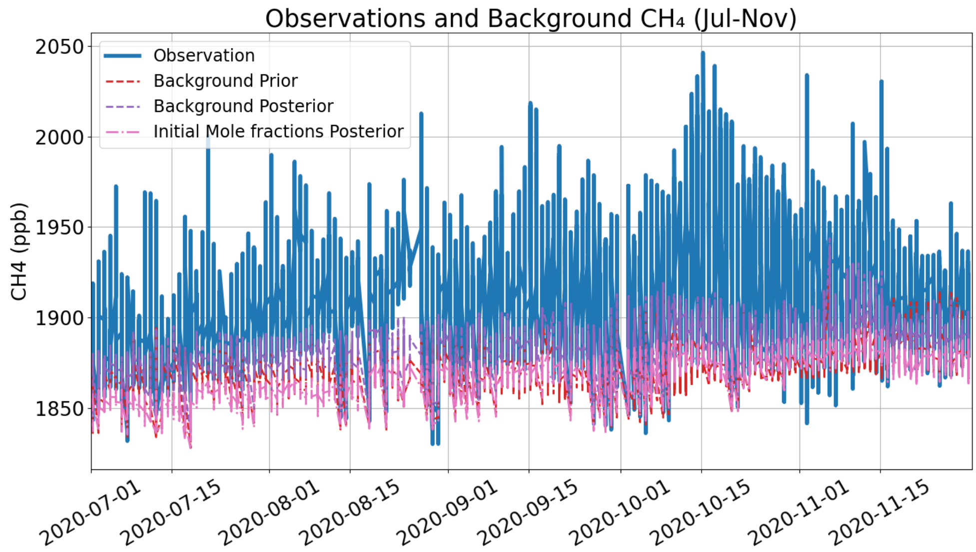

Figure S6. Time series of observed XCH_4 (blue) and modeled background mole fractions for July–November 2020 shown without temporal averaging. The red dashed line represents the prior background, the purple dashed line the posterior optimized background, and the pink dash-dotted line the optimized initial mole fraction component.

From the Figure S6, we can see that the posterior background for Jul-Nov follows the observation and there are observations available that are representative of background conditions. Also, since the prescribed uncertainties for the background are 0.3% to 0.7% (in the same order of magnitude of RMSD of the EGG4 background fields against co-located Tropomi observations), which constrains the inversion from making unrealistically large adjustments to the background field. As a consequence, even in a month like August when the observation – background differences are larger, the inversion preferentially corrects surface fluxes rather than attributing the mismatch largely to the background. In this sense, the background is only moderately adjustable and cannot compensate for large systematic discrepancies.

We also tested CAMS global inversion-optimized methane concentrations as an alternative background field. When evaluated at TROPOMI co-location points globally, the CAMS column concentrations show a large and systematic low bias. This suggests that the CAMS dataset is not suitable for providing the background for the inversions. In fact, when propagated through the FLEXPART background sensitivities, the resulting model background columns over the study region are typically 30–80 ppb lower than the TROPOMI XCH_4 values on many days (Figure S7). Using such a low-biased background would require the inversion to introduce unrealistically large positive background adjustments to match the observations or force compensation through excessive flux increments.

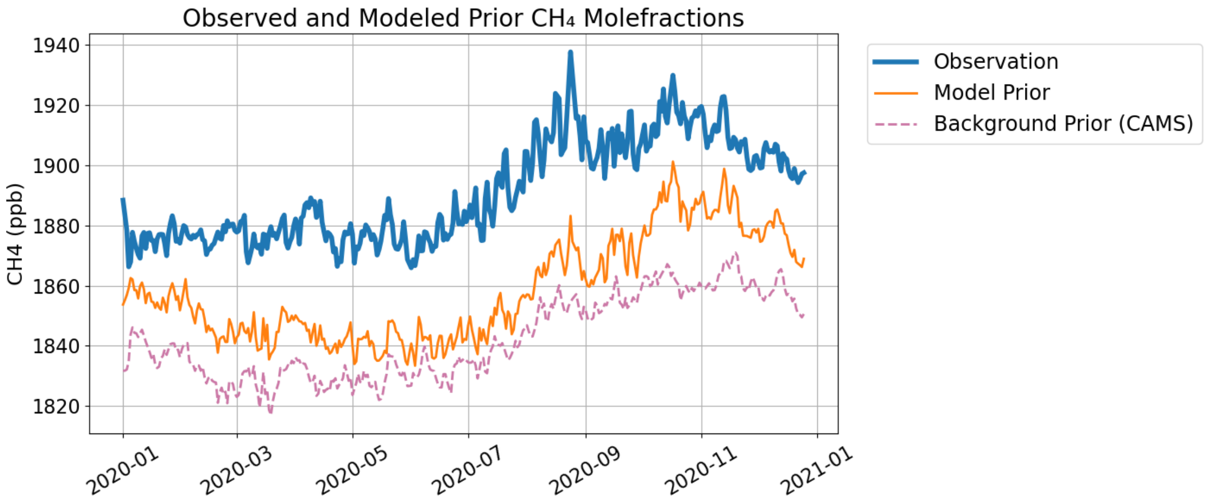

Figure S7. Time series of observed and modeled prior CH_4 column mole fractions over South Asia, highlighting the modeled background (dashed pink line) derived from CAMS data.

Thus, EGG4 was the best available data at the time for our inversion and for these reasons, EGG4 was selected as the background field. We further note that although regional emissions can influence the background signal the background adjustments remain within the prescribed uncertainty range. This indicates that the inversion does not attribute the seasonal enhancement primarily to boundary conditions but instead to regional surface fluxes, which is physically consistent with enhanced monsoon-driven wetland and agricultural emissions during July–November.
Overall, while boundary conditions can in principle alias with emissions, our tests with alternative background datasets and error settings indicate that the derived seasonal and spatial emission patterns remain robust and they are not primarily driven by background assumptions.

Specific comments:

Page 1, line 35-36: Soften to 'economic growth could cause…|"

Done!

Page 2, lines 43-47 and Figure 1: Make clear which BUR reports these are from

Added this.

Page 3, lines 64-65: There should be some mention in the introduction about the challenges of assimilating satellite observations, for example known biases, albedo-effects, lower signal-to-noise in a column versus a point in the boundary layer. This is lacking at present.

Added:

Satellite retrievals of methane are known to have systematic biases that vary by instrument, retrieval methodology and region, driven by factors such as surface albedo, aerosols, and thin clouds. Over Asia, these effects have been shown to translate into substantial differences in inferred emissions, with GOSAT and TROPOMI based inversions differing by up to 7.7 Tg yr^{-1} over northern India and eastern China (Liang et al., 2023). Biases associated with surface reflectance, aerosol loading, and across-track striping in early TROPOMI products can exceed 10 ppb in some regions and have been linked to false methane anomalies caused by unmodelled surface spectral features or inadequate topographic information (Balasus et al., 2023; Jongaramrungruang et al., 2021; Lorente et al., 2023). Algorithm updates to the operational TROPOMI retrieval have substantially reduced albedo-dependent biases through improved spectroscopy, higher-resolution surface altitude data, and posteriori corrections (Lorente et al., 2021). The scientific TROPOMI WFMD product further addresses these issues by using higher-order polynomial fitting to better represent spectral albedo variability, updated digital elevation models, refined machine-learning based quality filtering, and orbit-wise destriping and calibration, resulting in reduced systematic errors and improved spatiotemporal consistency. Notably, persistent seasonal biases present in the operational product at high latitudes are largely absent in WFMD (Lindqvist et al., 2024; Schneising et al., 2023).

Despite these advances, assimilating satellite column observations into inverse modeling systems remains challenging because column-averaged XCH_4 measurements have lower signal-to-noise ratio and weaker sensitivity to near-surface emissions compared to the in situ boundary-layer observations (Kuze et al., 2020) and their interpretation relies on accurate treatment of averaging kernels and prior vertical profiles. In addition, detection sensitivity is highly complex and influenced by water vapor, aerosol loading, planetary boundary layer structure, and illumination geometry. Current satellite instruments have detection thresholds of roughly 100–10,000 kg h^{-1}, which limits their precision relative to localized point-source measurements (Jacob et al., 2022). On the other hand, the number of satellite observations is much larger than that of in-situ measurements, and their spatial distribution more suitable for inverse modelling.

Page 3, line 66: also lacks any discussion of previous work using satellite (including TROPOMI) observations with Lagrangian models

Added:

Inverse modelling using satellite observations in combination with Lagrangian transport models has emerged as a powerful approach for refining regional and global greenhouse gas emission estimates. Recent studies demonstrate the ability of such frameworks to reveal systematic biases in prior emission estimates and to better resolve regional emission processes. Li et al., 2024 combined TROPOMI column methane observations with the

STILT Lagrangian transport model (Wu et al., 2018) and wetland model information to show that dry-season (May-July) wetland CH_4 emissions from the Pantanal (a large tropical wetland) are underestimated by a factor of 2 to 3 in commonly used models. A key early example over India is Ganesan et al., 2017, who combined GOSAT XCH_4 retrievals with surface and aircraft measurements and a Lagrangian framework to infer emissions at sub-national scales and assess trends during 2010–2015. They calculated the source-receptor relationships by running the NAME Lagrangian transport model (Jones et al., 2007) in backward mode for individual satellite retrievals and extend the framework to column observations through explicit application of averaging kernels and pressure weighting. Their results showed that Indian methane emissions during 2010–2015 were substantially lower than those reported by global inventories during that period and showed a pronounced monsoon-driven seasonal cycle, primarily linked to rice cultivation.

Our current study over SA will be an extension of this work in many ways. First, we employ the high-resolution TROPOMI satellite observations, which provide substantially denser spatial coverage than GOSAT, enabling a more detailed representation of spatial emission patterns across South Asia. Second, we integrate these observations within the FLEXPART–FLEXINVERT Lagrangian inversion framework, adopting the computationally efficient methodology introduced by Thompson et al., 2025 and allowing explicit treatment of column averaging kernels and background sensitivities within a high-resolution (0.5° × 0.5°) domain. In contrast to earlier GOSAT-based applications, we optimize both surface emissions and background concentrations in our inversion framework.

Page 4, line 102-104: Either replace Fig 2 with data after filtering or show an additional figure after filtering.

The aim is to show the TROPOMI column data and its coverage over South Asia as a whole. Now we have added an additional figure to show the data before and after filtering

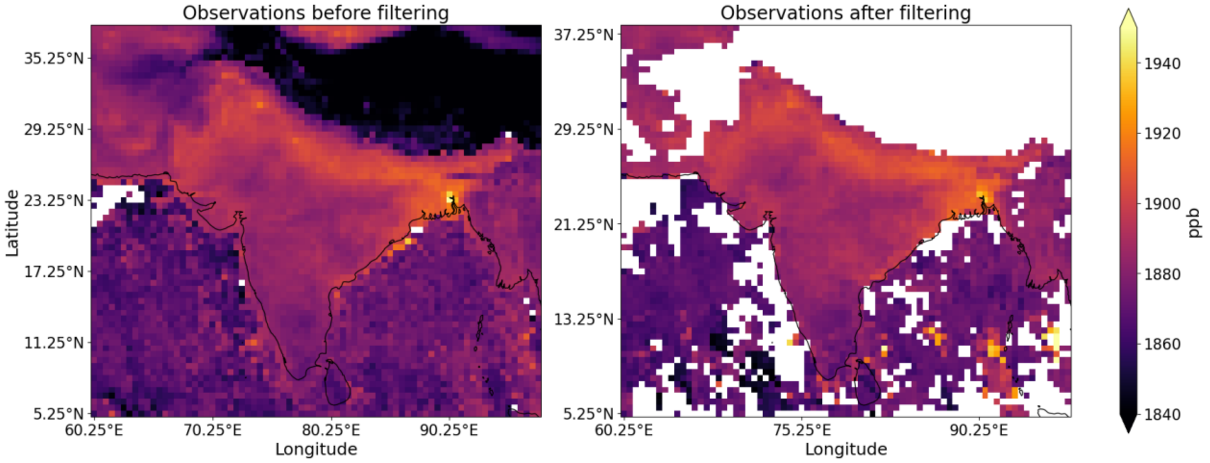

Figure S8. Spatial distribution of TROPOMI XCH_4 observations (ppb) over South Asia before (left) and after (right) quality filtering.

Page 4, lines 110-116: Is there any temporal averaging or is every day treated separately?

Days are treated separately. Retrievals are grouped and filtered within each day, and no averaging is performed across different days. The only temporal aggregation applied is within a day when multiple retrievals are spatially averaged into one release box.

Page 8, equation 1 and line 154-157: I don't follow the text that states that there are two components that make up the background term. The whole section only describes what sounds like the first component. It sounds as though these two terms are added but I don't follow this through Equation 1. Where are these two terms in Equation 1?

We are sorry for the confusion, the full equation for $\mathbf{y}^{\mathrm{model}}$ is

$$\mathbf{y}^{model} = \mathbf{Hf}_{\mathrm{in}} + \mathbf{Hf}_{\mathrm{out}} + \mathbf{H}^{ini}\mathbf{y}^{ini}$$

where $\mathbf{Hf}_{\mathrm{out}}$ is the boundary mole fraction or the contribution from the fluxes, but outside the inversion domain. This together with the initial mole fraction field (contribution from trajectory endpoints) forms the background field. As per the common practice seen in literature, both the $\mathbf{Hf}$ terms were put together as a single term for simplicity in equation 1.

Equation 1 and onward – are these matrices – bold font, etc?

We thank the reviewer for pointing this out. We have revised the notation to explicitly distinguish scalars from vectors and matrices using bold font.

Page 8, lines 159-162: how is it established that EGG4 has a smaller bias relative to TROPOMI? The conclusion that it is a robust background has not yet been established.

And

Page 8, line 164: I don't follow these numbers, -9.8 and 0.2. What CAMS data is being compared to? Is this surface data? There could still be a bias in the column? Please clarify this section.

We apologize for the lack of clarity. The comparison was performed at the column level by co-locating the CAMS inversion-optimized mole fraction product and the EGG4 reanalysis with the TROPOMI retrievals globally. The evaluation showed that the CAMS inversion-optimized product(v20r1) has a systematic negative bias relative to TROPOMI, whereas EGG4 shows substantially smaller mean bias. We have revised the manuscript to clarify that the comparison was performed using column-averaged mole fractions rather than surface concentrations and we removed the specific numerical bias values to avoid ambiguity.

As mentioned in the major comments (5), we have also calculated the model background mole fraction over the study domain using CAMS fields and then the model prior CH_4 based on this baseline (Equation 1). The details of this are answered in the major comments (5).

For generating initial mole fractions, we tested two global methane mole fraction products - CAMS global inversion-optimized greenhouse gas mole fractions, and the ECMWF Atmospheric Composition reanalysis EGG4, to identify the dataset that has the smaller bias relative to TROPOMI observations and thus provides a robust background for the inversion. The EGG4 dataset, which incorporates additional bias correction steps, demonstrated the smaller overall bias (mean bias error reduction of ~ 98% relative to CAMS data; MBE CAMS: -9.8 and MBE EGG4: 0.2) and was therefore adopted as the global initial mole fraction field.

Changed to:
To generate the initial mole fraction field for the inversion, we evaluated CAMS and EGG4 global methane concentration products for their consistency with the TROPOMI observations. The comparison was performed by co-locating the model column-averaged methane with the satellite retrievals globally. Among the tested datasets, the CAMS global inversion-optimized mole fraction product(v20r1) showed a systematic negative bias relative to TROPOMI, whereas the EGG4 reanalysis dataset shows substantially smaller mean bias. Since EGG4 assimilates atmospheric methane observations and includes bias correction procedures, it provides a background field that is more consistent with the TROPOMI observations. We therefore adopted EGG4 as the initial mole fraction field for the inversion.

Equation 2: Do the FLEXPART simulations model all the way to the top of the atmosphere, i.e. all of the N levels in TROPOMI? If not, what modifications/assumptions are made? The earlier Thompson et al 2025 paper does not clarify this, unless I have missed it. We laid out all of the equations for a satellite/Lagrangian setup in our paper Ganesan et al., 2017 (even though this was not cited at all in Thompson et al., 2025…) and when using NAME, we were only able to (easily) extract/apply the met to a defined height and therefore had to account for this. It would be helpful for me to understand how FLEXPART is applied as this does have an impact on the modelled column.

Yes, the top most height in FLEXPART simulation is 50km which is less than ~1hPa and it covers all of the TROPOMI levels. We have used 30 vertical levels in the FLEXPART simulations, of which 21 levels are in the troposphere. We have now cited and discuss Ganesan et al., 2017 in more detail. Sorry again that we have missed that paper.

Page 9, line 190 – how are these 30000 particles distributed through the column?

Particles are distributed in each layer according to the averaging kernel sensitivities for that retrieval. Figure 5 shows an example of this.

Page 10, line 240 – how you handle or interpret negative fluxes?

Negative fluxes after inversions were very small (~0.3 Tg/month). So, we didn't apply any non-negativity constraints for this study.

Page 18, line 413-414 – more could be done to discuss the "value of assimilating satellite observations" by comparing/understanding differences with Ganesan et al., 2017 and other studies within India. See major comment above.

We have now included in introduction section, how this work is an extension of Ganesan et al., 2017 and in what ways. We have also extended the comparison of our results to those of other studies.

Fig 7 – Why are there dropouts in the data/modelled mole fractions that are less than the boundary conditions?

Modelled mole fractions cannot be less than the background. The background concentrations are derived from large-scale reanalysis fields (EGG4) propagated using FLEXPART backward trajectories. It represents a smoothed large-scale field rather than a local air-mass measurement. In the inversion, the background scalars are optimized across four latitude bands (90°–30°N, 30°–0°N, 0°–30°S, and 30°–90°S) and three vertical layers (0–2000 m, 2000–10,000 m, and 10,000–50,000 m) and on a 30-day timescale. Because the background adjustment is coarser and the individual satellite retrievals, however, are sensitive to localized air masses, short-term advection of relatively cleaner into the domain can temporarily produce column values lower than the background. These occasional dropouts are isolated events and may reflect short-term noises that are not resolved by the coarse background optimization.

Fig 7 – It would be useful to see this plot for all of the individual data points in the inversion (which in my experience of using TROPOMI has a lot of scatter) because this current view shows everything after averaging across South Asia. There are a lot of data points, but you could show Jan and August for example.

Added in Supplementary figure, (a) for January and (b) for August

a)

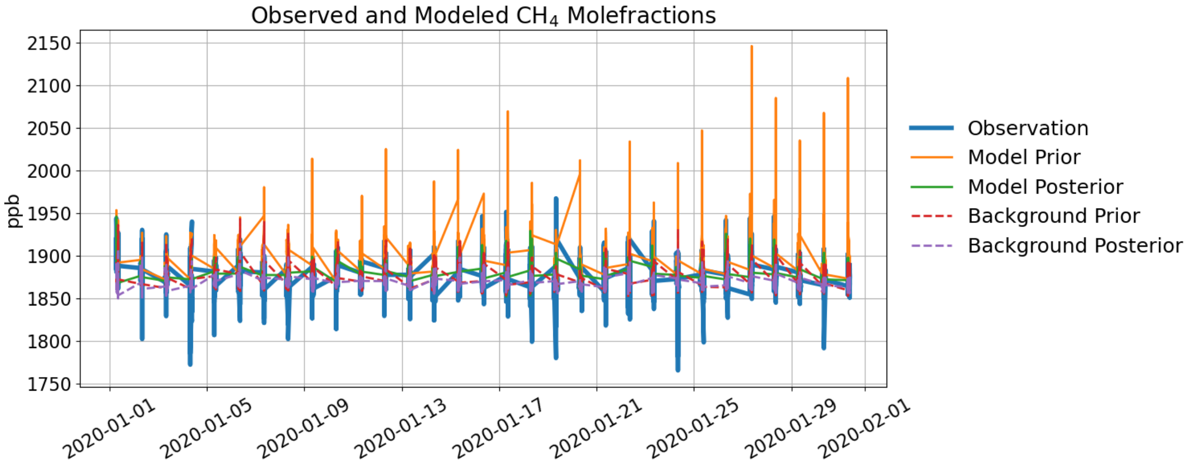

b)

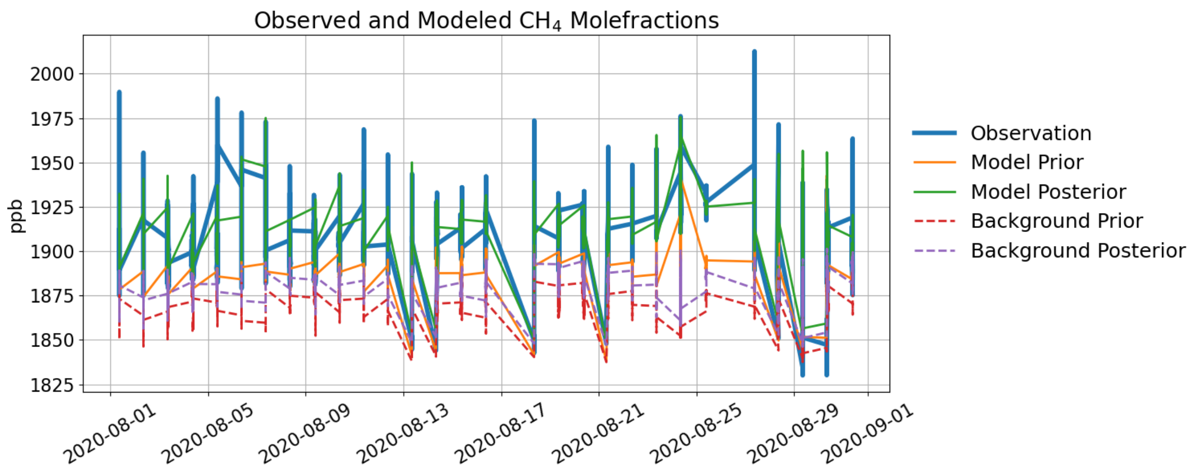

Figure S9: Comparison of observed and modeled CH_4 mole fractions (ppb) for all individual satellite retrievals used in the inversion during (a) January 2020 and (b) August 2020.

Fig 7 - Where is the associated timeseries of monthly emissions?

The monthly emissions are shown in figure 10 together with the hydrological variables in order to avoid duplication. We have now included the seasonal emissions as an additional figure.

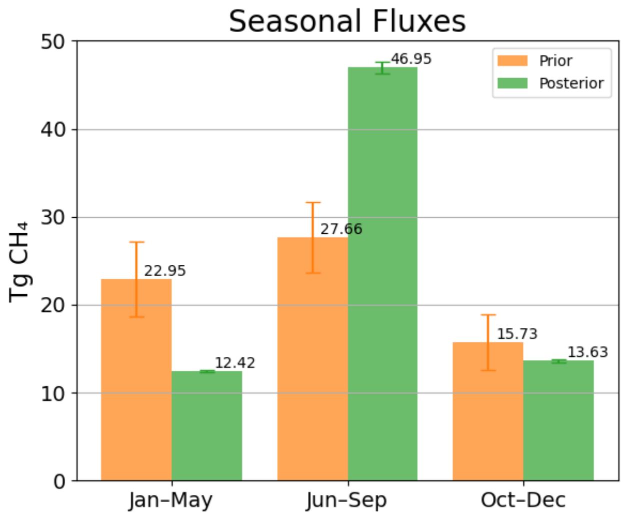

Figure S10: Seasonal methane fluxes (Tg CH_4) over South Asia for three periods (Jan–May, Jun–Sep, Oct–Dec), comparing inventory-based estimates (orange bars) with inversion-optimized fluxes (green bars). Error bars indicate the corresponding uncertainty ranges.

Table 2 (and Supp Fig 2) - The errorbars on the posteriors are very small…It is highly unlikely in my opinion that annual emissions (36.62) have uncertainties of 0.47 Tg/yr. On a national scale, the uncertainties on the prior are 2.54 Tg/yr. I think this needs to be thought through – are these numbers realistic?

Thanks for pointing this out. In our earlier calculations, the error cross-correlations where not considered when deriving uncertainties, which leads to an underestimate of aggregated uncertainty. The updated analysis includes cross-correlation terms, resulting in more realistic and slightly higher prior (66.34 ± 6.65 Tg yr^{-1}) and posterior (73.01 ± 0.7 Tg yr^{-1}) uncertainty estimates. The smaller uncertainty of the posterior fluxes reflects the stronger constraint provided by the TROPOMI observations. Many recent studies use other methods such as Monte-Carlo ensembles, which tend to give wider uncertainty ranges but we haven't done that for this study.

Table 2 and throughout – are presenting results to two decimal places warranted?

For India, two decimal places are probably not warranted. On the other hand, for countries like Sri Lanka, these are needed to provide meaningful information. For consistency, we have thus chosen to report results with two decimal places for all countries.

Figure 9 – there are no error bars in panel b.

Added!

Page 14, lines 319-327: I am confused with the interpretation. This shows that the UIB has the dual peak in runoff and not the LIB, due to irrigation? But why are the inversion fluxes showing the dual peak in the LIB? It looks like different regions are being compared? Please check the language and clarify. I would also caution against over-interpreting given this is one year of analysis. It would possibly be more robust if this was done over several years.

To clarify: the dual peak in runoff is observed in UIB, while the LIB does not show a similarly clear dual-peak runoff structure. In the inversion results, a dual peak structure in methane flux appears in both regions, but it is much more pronounced over the LIB. Over the UIB, the posterior flux shows only a modest seasonal variability compared to the relatively flat prior, and the dual peak is less prominent than in the LIB.

We also note that an independent inversion study (Liang et al., 2023) reports spatial emission increments over similar regions for the year 2019, suggesting that elevated emissions in this area are not unique to our analysis. Moreover, as clarified early in the major comments 4, our analysis of the runoff data for the year 2019 also shows the dual peak in runoff in UIB. The absence of this signal in LIB could be due to the missing data or processes in the runoff product (e.g., irrigation or regulated water releases) which are particularly important in the lower basin. We agree that more years of model results would have refined these findings.

Page 14, line 330-333: I caution against over-interpreting results. Individual grid cells will have very large uncertainty and looking at a single month of a single year, I think statements like this should be removed.

Further, the grid cell corresponding to Karachi, Pakistan, also shows a positive increment, with the highest posterior CH4 emissions occurring in September. Interestingly, this coincides with record monsoonal rainfall that caused severe flooding in Karachi during late August 2020.

Changed to:

Further, the grid cell encompassing Karachi, Pakistan, shows a positive posterior increment, with highest posterior methane emissions in September. Although this timing coincides with the late-monsoon period and Karachi flooding in 2020, given the large uncertainties at the grid-cell scale and the limited temporal coverage, no direct attribution to individual hydrometeorological events can be made.

Page 16, lines 360-367: The statistical relationships are very weak with one year of data. The conclusion that there is a "systematic enhancement…between fluxes and hydrological variability" is not supported with this dataset. See major comments.

We agree that the original wording overstated the strength of inference that can be drawn from a single year of monthly correlations. We have therefore revised the text to remove the term "systematic enhancement" and rewrite it in a suggestive tone.

Together, these results indicate a systematic enhancement in the linear relationship between the posterior methane fluxes and hydrological variability.

Changed to:

Together, these results suggest that the inversion tends to increase the consistency between methane flux variability and hydrological drivers compared to the prior. While the absolute correlations remain modest and the analysis is limited to a single year, the coherent increases across multiple hydrological variables indicate a plausible hydrological imprint on the posterior fluxes, warranting further investigation using longer time series.

3.2 Validation

To assess the robustness of the inversion results, lacking surface observations in South Asia, we performed an independent validation using the GOSAT–TROPOMI blended XCH_4 dataset (Balasus et al., 2023). This relatively recent product combines TROPOMI and GOSAT XCH4 retrievals using a machine-learning bias-correction framework designed to reduce the systematic biases between the two satellite instruments relative to ground truth and to improve spatial consistency. The dataset is publicly available and has already been used in several studies to infer methane emissions. Importantly, it is developed independently of the WFMD TROPOMI retrievals used in our inversion, thereby providing a fully external and independent consistency check of the posterior solution.

Figure S11 shows the time series of domain averaged column mean methane concentrations for 2020, comparing the prior model simulation, the posterior model simulation, and the blended GOSAT–TROPOMI observations. The prior simulation systematically underestimates methane concentrations during the monsoon and post-monsoon months (Jun-Nov), while slightly overestimating concentrations during the pre-monsoon period (Jan-May). This behavior is consistent with the seasonal flux adjustments inferred by the inversion, where prior emissions were found to be too low in the second half of the year and too high in the first half. The posterior simulation shows a clear improvement in capturing both the seasonal amplitude and the temporal variability of the observations, although a slight overestimation is seen overall. In particular, the enhanced concentrations during August-October are much better reproduced after inversion, indicating that the additional emissions inferred during the monsoon season are physically consistent with the observed atmospheric signal.

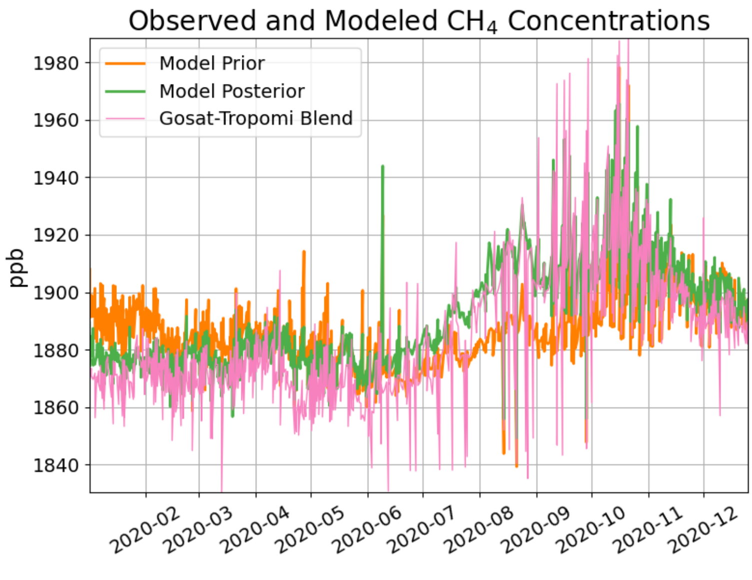

Figure S11. Domain-averaged prior and posterior modeled CH_4 concentrations compared with the GOSAT–TROPOMI blended XCH_4 dataset.

The improvement is further quantified in Figure S12, which shows the (a) RMSE and (b) MBE between modeled and blended XCH_4 for three seasonal groupings: January–May, June–September, and October–December.

For January–May, the RMSE decreases from 15.94 ppb (prior) to 9.77 ppb (posterior), corresponding to a reduction of 6.18 ppb or 38.7%. During the monsoon season (June–September), where the largest seasonal mismatch was observed in the prior simulation, the RMSE decreases from 19.01 ppb to 12.07 ppb, representing a reduction of 6.93 ppb or 36.5%. This is the largest absolute RMSE improvement and confirms that the inversion effectively corrects the strong underestimation of methane during the monsoon period. For October–December, the improvement is smaller, with RMSE decreasing from 10.09 ppb to 9.86 ppb (a reduction of 0.24 ppb, or 2.3%), indicating that the prior simulation was already relatively consistent with observations during this period. Overall, the posterior simulation consistently reduces the error relative to the independent blended dataset, with the most pronounced improvements occurring during the monsoon season.

For January–May, the prior simulation shows a strong positive bias of +13.98 ppb, which is reduced to +7.07 ppb in the posterior simulation. This corresponds to a bias reduction of 6.91 ppb (~49% reduction), indicating that the inversion corrects the prior overestimation during the pre-monsoon season. During June–September, the prior simulation shows a pronounced negative bias of −10.49 ppb, reflecting the underestimation of emissions. After inversion, the bias shifts to +4.61 ppb, reversing the sign of the bias but reducing its magnitude relative to the observations. For October–December, the prior bias is nearly neutral (−0.21 ppb), while the posterior shows a positive bias (+6.97 ppb). Although this increases the mean bias during this period, the RMSE remains largely unchanged, indicating that variability is still well represented.

Overall, the independent validation with the blended GOSAT–TROPOMI dataset demonstrates that the posterior solution improves both variance-based (RMSE) and mean-state (MBE) agreement with observations, increasing confidence in the inferred seasonal methane flux corrections.

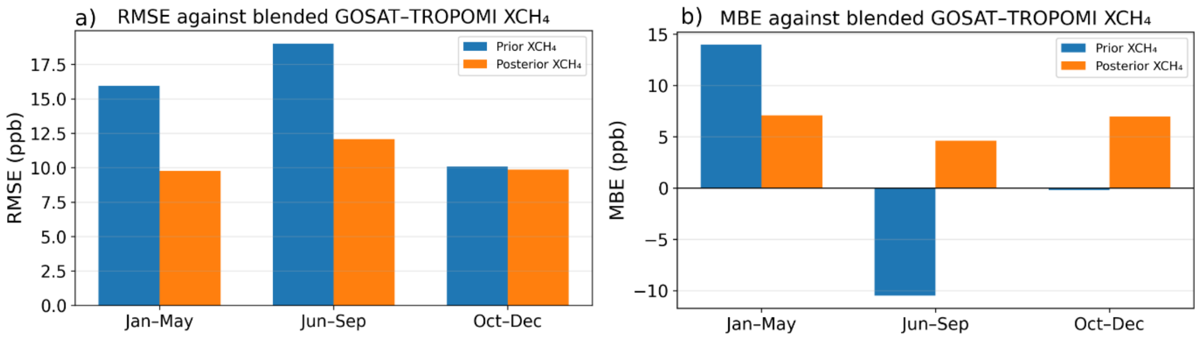

Figure S12. Seasonal RMSE (a) and MBE (b) of prior and posterior modeled XCH_4 relative to GOSAT–TROPOMI blended dataset. Statistics are shown for January–May, June–September, and October–December. Overall, the posterior simulation shows reduced errors and seasonal biases compared to the prior.

Reference

Anand, S., Dahiya, R. P., Talyan, V., and Vrat, P.: Investigations of methane emissions from rice cultivation in Indian context, Environment International, 31, 469–482, https://doi.org/10.1016/j.envint.2004.10.016, 2005.

Baig, S., Sayama, T., and Yamada, M.: Quantifying the changes in the runoff and its components across the Upper Indus River Basin under climate change, Journal of Water and Climate Change, 13, 3416–3434, https://doi.org/10.2166/wcc.2022.153, 2022.

Balasus, N., Jacob, D. J., Lorente, A., Maasakkers, J. D., Parker, R. J., Boesch, H., Chen, Z., Kelp, M. M., Nesser, H., and Varon, D. J.: A blended TROPOMI+GOSAT satellite data product for atmospheric methane using machine learning to correct retrieval biases, Atmospheric Measurement Techniques, 16, 3787–3807, https://doi.org/10.5194/amt-16-3787-2023, 2023.

Bovensmann, H., Burrows, J. P., Buchwitz, M., Frerick, J., Noël, S., Rozanov, V. V., Chance, K. V., and Goede, A. P. H.: SCIAMACHY: Mission Objectives and Measurement Modes, Journal of the Atmospheric Sciences, 56, 127–150, https://doi.org/10.1175/1520-0469(1999)056%253C0127:SMOAMM%253E2.0.CO;2, 1999.

Chandra, N., Patra, P. K., Bisht, J. S. H., Ito, A., Umezawa, T., Saigusa, N., Morimoto, S., Aoki, S., Janssens-Maenhout, G., Fujita, R., Takigawa, M., Watanabe, S., Saitoh, N., and Canadell, J. G.: Emissions from the Oil and Gas Sectors, Coal Mining and Ruminant Farming Drive Methane Growth over the Past Three Decades, Journal of the Meteorological Society of Japan. Ser. II, 99, 309–337, https://doi.org/10.2151/jmsj.2021-015, 2021.

Chen, A., Zhang, Z., Poulter, B., Feng, L., Liu, H., Murray, L. T., Yu, X., Huang, Z., Gaeta, D. C., Morgan, K. L., Zhu, Q., and Miller, S. M.: Spatial and Temporal Distribution of Global Wetland Methane Emissions During 2019–2020 Estimated From Satellite Observations, Journal of Geophysical Research: Atmospheres, 130, e2025JD044354, https://doi.org/10.1029/2025JD044354, 2025.

Dogniaux, M., Maasakkers, J. D., Girard, M., Jervis, D., McKeever, J., Schuit, B. J., Sharma, S., Lopez-Noreña, A., Varon, D. J., and Aben, I.: Global satellite survey reveals uncertainty in landfill methane emissions, Nature, 647, 397–402, https://doi.org/10.1038/s41586-025-09683-8, 2025.

Ganesan, A. L., Rigby, M., Lunt, M. F., Parker, R. J., Boesch, H., Goulding, N., Umezawa, T., Zahn, A., Chatterjee, A., Prinn, R. G., Tiwari, Y. K., Van Der Schoot, M., and Krummel, P. B.: Atmospheric observations show accurate reporting and little growth in India's methane emissions, Nat Commun, 8, 836, https://doi.org/10.1038/s41467-017-00994-7, 2017.

Gupta, D. K., Bhatia, A., Kumar, A., Chakrabarti, B., Jain, N., and Pathak, H.: Global warming potential of rice (Oryza sativa)-wheat (Triticum aestivum) cropping system of the Indo-Gangetic Plains, Indian J Agri Sci, 85, 807–816, https://doi.org/10.56093/ijas.v85i6.49243, 2015.

Hu, H., Hasekamp, O., Butz, A., Galli, A., Landgraf, J., Aan de Brugh, J., Borsdorff, T., Scheepmaker, R., and Aben, I.: The operational methane retrieval algorithm for TROPOMI, Atmospheric Measurement Techniques, 9, 5423–5440, https://doi.org/10.5194/amt-9-5423-2016, 2016.

International Energy Agency: Methane and climate change – Methane Tracker 2021, https://www.iea.org/reports/methane-tracker-2021/methane-and-climate-change, 2021.

Jacob, D. J., Varon, D. J., Cusworth, D. H., Dennison, P. E., Frankenberg, C., Gautam, R., Guanter, L., Kelley, J., McKeever, J., Ott, L. E., Poulter, B., Qu, Z., Thorpe, A. K., Worden, J. R., and Duren, R. M.: Quantifying methane emissions from the global scale down to point sources using satellite observations of atmospheric methane, Atmospheric Chemistry and Physics, 22, 9617–9646, https://doi.org/10.5194/acp-22-9617-2022, 2022.

Janardanan, R., Maksyutov, S., Tsuruta, A., Wang, F., Tiwari, Y. K., Valsala, V., Ito, A., Yoshida, Y., Kaiser, J. W., Janssens-Maenhout, G., Arshinov, M., Sasakawa, M., Tohjima, Y., Worthy, D. E. J., Dlugokencky, E. J., Ramonet, M., Arduini, J., Lavric, J. V., Piacentino, S., Krummel, P. B., Langenfelds, R. L., Mammarella, I., and Matsunaga, T.: Country-Scale Analysis of Methane Emissions with a High-Resolution Inverse Model Using GOSAT and Surface Observations, Remote Sensing, 12, 375, https://doi.org/10.3390/rs12030375, 2020.

Jones, A., Thomson, D., Hort, M., and Devenish, B.: The U.K. Met Office's Next-Generation Atmospheric Dispersion Model, NAME III, in: Air Pollution Modeling and Its Application XVII, 580–589, https://doi.org/10.1007/978-0-387-68854-1_62, 2007.

Jongaramrungruang, S., Matheou, G., Thorpe, A. K., Zeng, Z.-C., and Frankenberg, C.: Remote sensing of methane plumes: instrument tradeoff analysis for detecting and quantifying local sources at global scale, Atmospheric Measurement Techniques, 14, 7999–8017, https://doi.org/10.5194/amt-14-7999-2021, 2021.

Kuze, A., Suto, H., Nakajima, M., and Hamazaki, T.: Thermal and near infrared sensor for carbon observation Fourier-transform spectrometer on the Greenhouse Gases Observing Satellite for greenhouse gases monitoring, Appl. Opt., AO, 48, 6716–6733, https://doi.org/10.1364/AO.48.006716, 2009.

Kuze, A., Kikuchi, N., Kataoka, F., Suto, H., Shiomi, K., and Kondo, Y.: Detection of Methane Emission from a Local Source Using GOSAT Target Observations, Remote Sensing, 12, 267, https://doi.org/10.3390/rs12020267, 2020.

Lama, S., Maasakkers, J. D., Zhang, X., Girard, M., Dutt, S., Nandgaonkar, S., Varon, D. J., Sulprizio, M. P., Estrada, L. A., Balasus, N., Parker, R. J., Terao, Y., and Aben, I.: Evaluating national, state, and urban Indian methane emissions using satellites, EGUsphere, 1–36, https://doi.org/10.5194/egusphere-2025-6528, 2026.

Li, M., Kort, E. A., Bloom, A. A., Wu, D., Plant, G., Gerlein-Safdi, C., and Pu, T.: Underestimated Dry Season Methane Emissions from Wetlands in the Pantanal, Environ. Sci. Technol., 58, 3278–3287, https://doi.org/10.1021/acs.est.3c09250, 2024.

Liang, R., Zhang, Y., Chen, W., Zhang, P., Liu, J., Chen, C., Mao, H., Shen, G., Qu, Z., Chen, Z., Zhou, M., Wang, P., Parker, R. J., Boesch, H., Lorente, A., Maasakkers, J. D., and Aben, I.: East Asian methane emissions inferred from high-resolution inversions of GOSAT and TROPOMI observations: a comparative and evaluative analysis, Atmospheric Chemistry and Physics, 23, 8039–8057, https://doi.org/10.5194/acp-23-8039-2023, 2023.

Lindqvist, H., Kivimäki, E., Häkkilä, T., Tsuruta, A., Schneising, O., Buchwitz, M., Lorente, A., Martinez Velarte, M., Borsdorff, T., Alberti, C., Backman, L., Buschmann, M., Chen, H., Dubravica, D., Hase, F., Heikkinen, P., Karppinen, T., Kivi, R., McGee, E., Notholt, J., Rautiainen, K., Roche, S., Simpson, W., Strong, K., Tu, Q., Wunch, D., Aalto, T., and Tamminen, J.: Evaluation of Sentinel-5P TROPOMI Methane Observations at Northern High Latitudes, Remote Sensing, 16, 2979, https://doi.org/10.3390/rs16162979, 2024.

Lorente, A., Borsdorff, T., Butz, A., Hasekamp, O., aan de Brugh, J., Schneider, A., Wu, L., Hase, F., Kivi, R., Wunch, D., Pollard, D. F., Shiomi, K., Deutscher, N. M., Velazco, V. A., Roehl, C. M., Wennberg, P. O., Warneke, T., and Landgraf, J.: Methane retrieved from TROPOMI: improvement of the data product and validation of the first 2 years of measurements, Atmospheric Measurement Techniques, 14, 665–684, https://doi.org/10.5194/amt-14-665-2021, 2021.

Lorente, A., Borsdorff, T., Martinez-Velarte, M. C., and Landgraf, J.: Accounting for surface reflectance spectral features in TROPOMI methane retrievals, Atmos. Meas. Tech., 16, 1597–1608, https://doi.org/10.5194/amt-16-1597-2023, 2023.

Manjunath, K. R., Panigrahy, S., Kumari, K., Adhya, T. K., and Parihar, J. S.: Spatiotemporal modelling of methane flux from the rice fields of India using remote sensing and GIS, International Journal of Remote Sensing, 27, 4701–4707, https://doi.org/10.1080/01431160600702350, 2006.

Matthews, E., Fung, I., and Lerner, J.: Methane emission from rice cultivation: Geographic and seasonal distribution of cultivated areas and emissions, Global Biogeochemical Cycles, 5, 3–24, https://doi.org/10.1029/90GB02311, 1991.

Miller, S. M., Michalak, A. M., Detmers, R. G., Hasekamp, O. P., Bruhwiler, L. M. P., and Schwietzke, S.: China's coal mine methane regulations have not curbed growing emissions, Nat Commun, 10, 303, https://doi.org/10.1038/s41467-018-07891-7, 2019.

Schneising, O., Buchwitz, M., Hachmeister, J., Vanselow, S., Reuter, M., Buschmann, M., Bovensmann, H., and Burrows, J. P.: Advances in retrieving XCH_4 and XCO from Sentinel-5 Precursor: improvements in the scientific TROPOMI/WFMD algorithm, Atmospheric Measurement Techniques, 16, 669–694, https://doi.org/10.5194/amt-16-669-2023, 2023.

Singh, A., Kuttippurath, J., Abbhishek, K., Mallick, N., Raj, S., Chander, G., and Dixit, S.: Biogenic link to the recent increase in atmospheric methane over India, Journal of Environmental Management, 289, 112526, https://doi.org/10.1016/j.jenvman.2021.112526, 2021.

Thompson, R. L., Krishnankutty, N., Pisso, I., Schneider, P., Stebel, K., Sasakawa, M., Stohl, A., and Platt, S. M.: Efficient use of a Lagrangian particle dispersion model for atmospheric inversions using satellite observations of column mixing ratios, Atmospheric Chemistry and Physics, 25, 12737–12751, https://doi.org/10.5194/acp-25-12737-2025, 2025.

Toha, M., Ariyan, T. N., and Alam, M.: Methane hotspots in landfills: A systematic review on transboundary dispersion and impacts on heatwaves in South Asia, Cleaner Waste Systems, 10, 100235, https://doi.org/10.1016/j.clwas.2025.100235, 2025.

Worden, J. R., Cusworth, D. H., Qu, Z., Yin, Y., Zhang, Y., Bloom, A. A., Ma, S., Byrne, B. K., Scarpelli, T., Maasakkers, J. D., Crisp, D., Duren, R., and Jacob, D. J.: The 2019 methane budget and uncertainties at 1° resolution and each country through Bayesian integration Of GOSAT total column methane data and a priori inventory estimates, Atmospheric Chemistry and Physics, 22, 6811–6841, https://doi.org/10.5194/acp-22-6811-2022, 2022.

Wu, D., Lin, J. C., Fasoli, B., Oda, T., Ye, X., Lauvaux, T., Yang, E. G., and Kort, E. A.: A Lagrangian approach towards extracting signals of urban CO_2 emissions from satellite observations of atmospheric column CO_2 (XCO_2): X-Stochastic Time-Inverted Lagrangian Transport model ("X-STILT v1"), Geoscientific Model Development, 11, 4843–4871, https://doi.org/10.5194/gmd-11-4843-2018, 2018.

Yu, X., Millet, D. B., Henze, D. K., Turner, A. J., Delgado, A. L., Bloom, A. A., and Sheng, J.: A high-resolution satellite-based map of global methane emissions reveals missing wetland, fossil fuel, and monsoon sources, Atmospheric Chemistry and Physics, 23, 3325–3346, https://doi.org/10.5194/acp-23-3325-2023, 2023.